Warming and environmental changes in the eastern North Sea Basin during the Palaeocene-Eocene Thermal Maximum as revealed by biomarker lipids

Petra L. Schoon[a] , Claus Heilmann-Clausen[b], Bo Pagh Schultz[c], Jaap S. Sinninghe Damsté[a], and Stefan Schouten[a,*]

[a]*NIOZ Royal Netherlands Institute for Sea Research, Department of Marine Organic Biogeochemistry, PO Box 59, 1790 AB Den Burg, The Netherlands*

[b]*Aarhus University, Department of Geoscience, Høegh-Guldbergs Gade 2, 8000 Aarhus C, Denmark*

[c]*MUSERUM, Havnevej 14, 7800 Skive, Denmark*

*Corresponding author: E-mail: stefan.schouten@nioz.nl

[a]*Present address:*
Department of Geology - Quaternary Sciences
Lund University
Sölvegatan 12, 22362 Lund
Sweden

Abstract

Analysis of sediments deposited at different latitudes around the world during the Palaeocene-Eocene Thermal Maximum (PETM; ~56 Ma) have revealed a globally profound warming phase, regionally varying from 5 to 8 °C. Such records from Europe have not yet been obtained. We studied the variations in sea surface and continental mean annual air temperatures (SST and MAT, respectively) and the distribution patterns and stable carbon isotopes of higher plant-derived *n*-alkanes in two proximal PETM sections (Fur and Store Bælt, Denmark) from the epicontinental North Sea Basin. A negative carbon isotope excursion (CIE) of 4-7 ‰ was recorded in land plant-derived *n*-alkanes, similar to what has been observed for other PETM sections. However, differences observed between the two proximal sites suggest that local factors, such as regional vegetation and precipitation patterns, also influenced the CIE. The presence of S-bound isorenieratene derivatives at the onset of the PETM and increased organic carbon contents points to a rapid shift in depositional environment; from well-oxygenated to anoxic and sulfidic. These euxinic conditions are comparable with those during the PETM in the Arctic Ocean. SSTs inferred from TEX_{86} show relatively low temperatures followed by an increase of ~7 ^{o}C across the PETM. At the Fur section, a remarkably similar temperature record was obtained for MAT using the MBT'/CBT proxy. However, the MAT record of the Store Bælt section did not reveal this warming.

Keywords: PETM, warming, CIE, *n*-alkanes, photic zone euxinia

1. Introduction

Climate conditions during the late Palaeocene and early Eocene were most likely the warmest of the Cenozoic Era (Zachos et al., 2001). Superimposed on the long-term Late Palaeocene – Early Eocene warming trend are transient intervals with rapid warming and environmental changes. The Palaeocene-Eocene Thermal Maximum (PETM, ~56 Ma) is the largest event and has been documented in sediments all over the world. Besides a major temperature increase, the PETM is characterized by other environmental and climate changes, such as the extinction of ca. 50% of benthic foraminiferal species (Sluijs et al., 2007a and references cited therein), and a decrease in water column oxygen concentrations in deep oceans, coastal settings and isolated basins (e.g. Sluijs et al., 2006 and 2014; Chun et al., 2010; Nicolo et al., 2010). It is further associated with a massive release of ^{13}C-depleted carbon to the oceans and atmosphere as reflected by a negative carbon isotope excursion (CIE) of >2.5 ‰ (e.g. Kennett and Stott, 1991; Schouten et al., 2007b; Sluijs et al., 2007a; McInerney and Wing, 2011).

Deep sea sediments have recorded a surface ocean warming of 4 to 8 °C (Fig. 1), based on the Mg/Ca ratio and δ^{18}O composition of planktonic foraminifera (Kennett and Stott, 1991; Thomas et al., 2002; Tripati and Elderfield, 2005; Zachos et al., 2003). Unfortunately, these records are often affected by redeposition of secondary calcite during early diagenesis (Pearson et al., 2001; Schrag, 1999) and carbonate dissolution due to the vertical progradation of the lysocline (Stap et al., 2009; Zachos et al., 2005; Zeebe and Zachos, 2007). Furthermore, the decrease in seawater pH, associated with the massive release of carbon to the oceans, may have increased δ^{18}O values causing a potential underestimation of PETM warming (Uchikawa and Zeebe, 2010).

The distribution of archaeal and bacterial glycerol dialkyl glycerol tetraethers (GDGTs) can also be used to infer sea surface temperature (SST), using the TEX_{86} proxy (Schouten et

al., 2002), and mean annual air temperature (MAT), using the MBT/CBT proxy (Weijers et al., 2007b; Peterse et al., 2012). So far, TEX_{86} palaeothermometry has been applied to a limited number of PETM sections (Hollis et al., 2012; Sluijs et al., 2006, 2007, 2011, 2014; Zachos et al., 2006) covering only a few locations worldwide, whereas a PETM MAT record based on the MBT/CBT proxy is available only for a single site located in the Arctic Ocean (Weijers et al., 2007a). The temperature records based on TEX_{86} show a similar extent of warming as those recorded by Mg/Ca and $\delta^{18}O$ of foraminifera, i.e. 5-8 ^{o}C (Fig. 1). Arctic continental air temperatures inferred from MBT/CBT values increased by about 6 ^{o}C (Fig. 1; Weijers et al., 2007a). Temperature records of the New Jersey continental margin, as well as of southern high latitudes, show a somewhat larger warming than most other temperature records (Fig. 1). However, global coverage of the existing PETM temperature records is still relatively poor, limiting the understanding of the underlying mechanisms of heat transport that drive greenhouse climates, such as during the PETM (cf. Huber and Caballero, 2011). In addition, most records are based on a single location which prohibits an assessment of local variability compared to imposed global changes. Recently, Caballero and Huber (2013) were able to model the high Eocene temperatures, but with some significant regional data-model discrepancies, emphasizing the importance of improving regional temperature proxy coverage.

In the eastern North Sea Basin, the PETM was previously identified by dinoflagellate stratigraphy and a 6-8 ‰ CIE in organic carbon (Heilmann-Clausen and Schmitz, 2000; Schmitz et al., 2004). Due to the close proximity to coastal areas it is likely that the sedimentary organic carbon contains large amounts of terrestrial organic matter, which may have a different stable carbon isotopic composition than marine organic matter (Bowen et al., 2004; Schouten et al., 2007b; Smith et al., 2007; Sluijs and Dickens, 2012). The relatively large CIE in organic carbon, compared to that in foraminiferal calcite (Dickens, 2011, and

references cited therein) may, therefore, be attributed to variations in the ratio of terrestrial to marine organic carbon (cf. Sluijs and Dickens, 2012). On the other hand, such a large CIE is also observed in land plant-derived *n*-alkanes at different PETM sites around the world (e.g. Handley et al., 2008; Pagani et al., 2006; Schouten et al., 2007b), and has led to the suggestion that the atmospheric CIE may have been larger than the generally accepted 2-3 ‰ recorded by marine calcite (Diefendorf et al., 2010; Handley et al., 2008, 2011; Pagani et al., 2006).

In this study, we present new organic geochemistry records from two nearby PETM sections in Denmark, situated in the eastern part of the North Sea Basin at the time of deposition (Fig. 2). We analysed the distribution of GDGTs to determine TEX_{86}-derived sea water and MBT/CBT-derived continental air temperatures thereby providing, to the best of our knowledge, the first European temperature records across the PETM. The aim of our study is to gain insight into the regional climate response of the carbon cycle perturbations during the PETM at this latitude, contributing to an improved geographic coverage of temperature proxy data for the Late Palaeocene – Early Eocene greenhouse climate. In addition, we analysed the distribution and stable carbon isotopic composition of higher plant biomarkers to constrain the terrestrial CIE.

2. Site descriptions and depositional setting

In this study, we used sediments from two sections in Denmark covering the Palaeocene-Eocene transition (Figs. 1 and 2). The study area is situated in the Norwegian-Danish Basin, a sub-basin of the larger, almost land-locked, epicontinental North Sea Basin. Water depths at the study sites during the late Palaeocene-early Eocene probably varied between upper bathyal and outer neritic (Heilmann-Clausen, 2006; Knox et al., 2010). Nearest coastlines were situated in southern Norway, northern Germany and in Sweden (Knox et al., 2010). Sea

level changes in the basin were probably caused mainly by phases of thermal subsidence and uplift due to varying activity of the Iceland mantle plume, and the onset of sea-floor spreading between Greenland and the British Isles-Norway (Knox, 1996a; Knox et al., 2010). The sedimentary succession of the late Palaeocene-early Eocene in Denmark consists of mainly hemipelagic mudstones and a local diatomite. A lithostratigraphic subdivision and mapping is provided by Heilmann-Clausen et al. (1985). A prominent series of volcanic ash layers is present in the earliest Eocene sediments. The ashes are subdivided into a lower series given negative numbers, and an upper positive series (Bøggild, 1918).

One of the sampled Palaeocene-Eocene sections was recovered in a core obtained from a borehole (D.G.I. 83101) drilled in 1983 in Store Bælt, the strait between the Danish islands Sjælland and Fyn. The position of the borehole is 55°N 21'N – 11° 05'E (Fig. 2). This section is one of the most continuous Palaeocene-Eocene records in Denmark (Nielsen et al., 1986). In this study, we analysed sediments of this core from 142.57 to 123.60 meters below sea floor (mbsf) covering 5 different lithological units. The late Palaeocene succession includes, in ascending order, the Holmehus Formation, the informal Østerrende Clay and the informal Glauconitic Silt unit (Nielsen et al., 1986). Above the latter unit follows the Ølst Formation, which belongs to the early Eocene (Heilmann-Clausen and Schmitz, 2000), and of which we only studied the lower part, i.e. the Haslund Member which corresponds to the negative numbered ash series of Bøggild (1918). The basal part of this member is referred to the informal Stolleklint Clay (Heilmann-Clausen, 1995). Our uppermost sample is from a level above the Stolleklint Clay (Figs. 3 and 4).

The Holmehus Formation consists of hemipelagic non-calcareous mudstones, with an overall high degree of bioturbation (Nielsen et al., 1986). The common *Zoophycos* burrows suggest an upper bathyal depositional environment (Bottjer and Droser, 1992). The Holmehus Formation is gradually overlain by the informal Østerrende Clay, which was deposited in a

more proximal setting, probably in somewhat shallower waters (Heilmann-Clausen, 1995; 2006). The Østerrende Clay is sharply overlain by the Glauconitic Silt of latest Palaeocene age. This unit is characterized as a clayey, sandy silt; the silt and sand mainly consist of biogenic and authigenic grains (Nielsen et al., 1986). The Glauconitic Silt includes a fauna with primitive forms of agglutinated foraminifers (Laursen and King, 1999) and was most likely deposited under low sedimentation rates in an upper bathyal or outer neritic environment. There is a distinct transition between the Glauconitic Silt and the lowermost Eocene Stolleklint Clay, which consists of finely laminated, non-calcareous clay. The lower boundary of the Stolleklint Clay is marked by a sharp negative isotope shift in total organic carbon (TOC) of ~6 ‰ at the base of the Stolleklint Clay between 133.24 and 132.53 mbsf (Heilmann-Clausen and Schmitz, 2000; Schmitz et al., 2004), concomitant with a sudden dominance of the dinocyst genus *Apectodinium* (Nielsen et al., 1986) marking the onset PETM.

The other studied section is a beach and cliff section at Stolleklint on the island Fur located in western Limfjorden, NW Denmark (Fig. 2; 56° 50' 28"N – 8° 59' 29"E). The lower part of this PETM section became exposed after a storm in 2005 and gave an opportunity for sampling across the Palaeocene/Eocene transition, which is placed at the base of the Stolleklint Clay. The Stolleklint Clay overlies a succession which can be correlated with the Østerrende Clay-Glauconitic Silt found in Store Bælt (Figs. 3 and 4). The preservation of an extremely fine lamination (Heilmann-Clausen, 2014) indicates a water depth deeper than storm wave base, probably outer neritic, 100-200 m. Like in Store Bælt, a sudden dominance of the dinocyst *Apectodinium* begins at the base of the Stolleklint Clay. Unfortunately, from ~2.5 m above the base of the Stolleklint Clay an interval with an estimated thickness of 10-20 m is partly unexposed and has been disturbed by the last glaciation. Above this interval follow undisturbed sediments representing the topmost ~3 m of the Stolleklint Clay, which are again

overlain by the Fur Formation (Fig. 3 and 4). The latter is a clayey diatomite intercalated with volcanic ash layers (Pedersen, 1981 Pedersen and Surlyk, 1983; Pedersen et al., 2004). The boundary between the Stolleklint Clay and the Fur Formation is placed at the thick white ash layer -33 (Heilmann-Clausen et al., 1985). The dominance of *Apectodinium* spp. continues a short distance above ash -33, i.e., into the basal few meters of the Fur Formation (Heilmann-Clausen, 1994). Previous results from two other sections in Denmark (Heilmann-Clausen and Schmitz, 2000; Schmitz et al., 2004) show that the dominance of *Apectodinium* closely corresponds to the CIE. The maximum of the CIE is, therefore, expected to be present in the glacially-disturbed interval. The top of the section here studied is at ash layer -17 in the lower part of the Fur Formation. Ash -17 is well above the zone with abundant *Apectodinium* (Heilmann-Clausen, 1994). Ash layer -17 was radiometrically dated at 55.12 ± 0.12 Ma (Storey et al., 2007). Dating the onset of the PETM is based on the extrapolation of the absolute age of this particular ash layer (Hilgen et al., 2010; Westerhold et al., 2009).

3. Methods

3.1 Bulk elemental and isotopic analysis

Prior to analysis, sediment samples from Store Bælt and Fur were freeze-dried and ground to a fine powder, partially using pestle and mortar and partially by means of a bowl mill. For the analysis of the total organic carbon (TOC) content and the stable carbon isotopic composition of TOC ($\delta^{13}C_{TOC}$), powdered sediment samples were acidified with 1M HCl for 12 h to remove all carbonate from the sediment matrix. Ca. 1.0 mg of decalcified sediment was weighed into a tinfoil cup and subsequently analysed on a Flash elemental analyser coupled to a ThermoFisher Delta^{plus} mass spectrometer. The instruments were calibrated against in-house standards. Duplicate runs showed a reproducibility of 0.1 % for TOC content and 0.1 ‰ for $\delta^{13}C_{TOC}$.

3.2 Extraction and fractionation

Total lipid extracts were obtained using a 9:1 (v/v) mixture of dichloromethane (DCM) and methanol (MeOH), at high temperature (100 ºC) and pressure (7.6×10^6 Pa) on a Dionex Accelerated Solvent Extractor (ASE). The extracts were then separated into an apolar and a polar fraction by means of column chromatography using an Al_2O_3 column and solvent mixtures of 9:1 (v/v) hexane:DCM, and 1:1 (v/v) DCM:MeOH, respectively. The apolar fractions were analysed for the distribution and stable carbon isotopic composition of land plant-derived *n*-alkanes. Prior to compound specific isotope analysis of *n*-alkanes, the unsaturated hydrocarbons were removed from the apolar fraction using a small column filled with Ag^+-impregnated silica and hexane as eluent. The polar fractions were analysed for GDGTs. Finally, sulfur-bound isorenieratane was analysed by desulfurization of an aliquot of the total extract using Raney Nickel as described previously by Schoon et al. (2011). The desulfurized extract was separated into an apolar and polar fraction as described above. The apolar fraction was analysed for the concentration of sulfur-bound isorenieratane.

3.3 GC, GC-MS and GC-irmMS analysis

Apolar fractions were analyzed on a HP 6890 gas chromatograph (GC) and on a Thermofinnigan TRACE GC coupled to a Thermofinnigan DSQ quadropole mass spectrometer (GC/MS) for biomarker lipid identification. Compound specific carbon isotope analyses were performed on a Finnigan Delta V isotope ratio mass spectrometer (IRMS) coupled to an Agilent 6890 GC. All GC, GC-MS, and GC-IRMS conditions are the same as described in Schoon et al. (2011). All stable carbon isotope values are reported in the $\delta^{13}C$ notation relative to the VPDB ^{13}C standard.

3.4. GDGT analysis

Polar fractions were dissolved in a hexane:propanol (99:1, v/v) solution and filtered over a 0.45 μm PTFE filter prior to analysis. Samples were analysed using high performance liquid chromatography/atmospheric pressure chemical ionization- mass spectrometry (HPLC/APCI-MS) according to Schouten et al. (2007a). We calculated TEX_{86} values according to Schouten et al. (2002). Several calibrations have been proposed to estimate sea water temperatures. Liu et al. (2009) proposed to use a non-linear inverse function for TEX_{86}: the $1/TEX_{86}$ ratio. This was later recalibrated by Kim et al. (2010), based on an extensive global core-top dataset. Kim et al. (2010) further used this extended dataset to develop two new SST calibrations: TEX_{86}^{H} and TEX_{86}^{L}. The TEX_{86}^{L} equation differs from the TEX_{86}^{H} equation, in that it excludes the crenarchaeol isomer, making it applicable for a temperature range that includes modern (sub)polar oceans with SST <15 °C. Application of the TEX_{86}^{H} to a PETM section in New Jersey led Kim et al. (2010) to recommend the use of this calibration for greenhouse worlds with SST >15 °C, whilst it is also correlated to a higher degree with SST than $1/TEX_{86}$. Therefore, TEX_{86}^{H} seems to be the most appropriate proxy to reconstruct temperature in this study. It has a calibration error of ±2.5 °C.

MAT estimates were calculated using the revised global MBT'/CBT calibration of Peterse et al. (2012), based on the relative distribution of soil-derived branched GDGTs (Weijers et al., 2007b). Additionally, we calculated the BIT index (Hopmans et al., 2004), which is the ratio between soil-derived branched GDGTs and aquatic crenarchaeol, and is a measure for the relative input of soil organic matter in marine sediments.

4. Results and Discussion

4.1 Magnitude of the CIE during the PETM

The TOC record of the Fur section shows overall low values (<0.6 %) for the Late Palaeocene sediments. At the onset of the CIE the TOC levels abruptly increase to up to 3.5 % (Fig. 3a). Coincident with this increase of TOC, a decrease of ~5 ‰ in $\delta^{13}C_{TOC}$ at the Fur section is recorded. Values for TOC content and $\delta^{13}C$ composition of the Store Bælt section were previously reported by Heilmann-Clausen and Schmitz (2000) and Schmitz et al. (2004) and show a similar pattern as for the Fur section: TOC content increases from <0.6% towards peak values of 5 % at 130.89 m depth (Fig. 3b), whereas the $\delta^{13}C_{TOC}$ record of the Store Bælt section shows a decrease of ~6 ‰ between 132.53 and 133.24 mbsf (Figs. 3a and b). The $\delta^{13}C_{TOC}$ profiles of both Danish sections follow the general shape that is often found in many marine and continental PETM sections (Sluijs et al., 2007a and references cited therein), i.e. a rapid onset followed by a plateau and a gradual decrease (Figs. 3a and b), although the glacially disturbed interval in the PETM section at the Fur section (Fig. 3a) partially masks the plateau of the CIE.

A CIE of 5-6 ‰ of the TOC falls into the range generally recorded worldwide, but is highly susceptible to variations in the ratio of terrestrial and marine derived organic matter (e.g. McInerney and Wing, 2011; Schouten et al., 2007b; Sluijs and Dickens, 2012). The distribution and stable carbon isotope values of long-chain *n*-alkanes were, therefore, also determined. Odd carbon numbered *n*-alkanes, generally in the range of 25 to 35 carbon atoms, are typically derived from epicuticular leaf waxes of higher land plants (Eglinton and Hamilton, 1967). Of the odd-carbon numbered *n*-alkanes, the C_{29} *n*-alkane is the most dominant in all sediments, followed by either the C_{27} or the C_{31} *n*-alkane. The carbon preference index (CPI) is a measurement to express the relative predominance of the odd-numbered *n*-alkanes (Bray and Evans, 1961; Marzi et al., 1993). The CPI values around the CIE of the Store Bælt section (~1.8) are lower than those at the Fur section (2-3), but are overall mostly well above 1 (up to 3.5; Figs. 3a and b), indicating a dominance of terrestrial-

derived odd-numbered long-chain *n*-alkanes. However, we cannot exclude a potential contribution of marine-derived even-numbered long chain *n*-alkanes which would lower the CPI index.

During the latest Palaeocene, *n*-alkane $\delta^{13}C$ values fluctuate around -29.5 ‰ for the *n*-C_{27} and *n*-C_{29} alkanes and around -30.5 ‰ for the *n*-C_{31} alkane for both sections (Figs. 3a and b). At the Fur section, the magnitude of the CIE in the *n*-alkanes ranges from 6.2 ‰ for the *n*-C_{27} and *n*-C_{31} alkanes to 6.7 ‰ for the *n*-C_{29} alkane (Fig. 3a). For the Store Bælt section, the $\delta^{13}C$ values of the *n*-C_{27}, *n*-C_{29}, and *n*-C_{31} alkanes decrease coincident with the CIE in TOC, by 5.7 ‰, 4.6 ‰, and 3.8 ‰ respectively (Fig. 3b). Most PETM sections record terrestrial CIEs in the range of 4-6 ‰ (e.g. McInerney and Wing, 2011), similar to that recorded for TOC and *n*-alkanes at the Store Bælt section. The decrease in $\delta^{13}C$ in the C_{27}-C_{31} *n*-alkanes at the Fur section is 1-2 ‰ larger, and appears to slightly precede the CIE in TOC. The smaller CIE in the *n*-alkanes observed at the Store Bælt section compared to the Fur section could be explained by a larger input of marine-derived *n*-alkanes (Pagani et al., 2006), which have a smaller CIE compared to terrestrial *n*-alkanes. This is evident by the higher relative abundance of shorter-chain *n*-alkanes, such as *n*-C_{17}, generally considered to derive from aquatic organisms (Han and Calvin, 1966), and also explains the relatively low CPI values at the Store Bælt section, indicating a more distal position of this location than the section at Fur.

Recently, Schoon et al. (2013) used the $\delta^{13}C$ values of crenarchaeol to reconstruct $\delta^{13}C$ records of marine dissolved inorganic carbon (DIC) in the same PETM sections as studied here. The $\delta^{13}C$ composition or crenarchaeol is thought be directly related to $\delta^{13}C$ of the dissolved inorganic carbon with a constant offset of ~20‰ (Könneke et al., 2012). The ~3.6 ‰ CIE recorded for crenarchaeol in the eastern North Sea Basin thus suggests a CIE of marine DIC of similar magnitude, although care has to be taken as the isotope systematics and

carbon metabolism of Thaumarchaeota and the impact of depth habitat of Thaumarchaeota on the $\delta^{13}C$ of crenarchaeol are poorly constrained. However, this value is consistent with the 3.0-3.5 ‰ CIE globally inferred from marine calcite and 1-3.5‰ lower than the CIE recorded in the C_{27}-C_{29} *n*-alkanes. Hence, also at the Danish PETM sites, the terrestrial CIE seems to be larger than the marine CIE.

The most important amplification mechanisms postulated to explain a larger terrestrial CIE in comparison to the marine CIE are an increase in relative humidity (Bowen et al., 2004), or a change in vegetational types (Schouten et al., 2007b; Smith et al., 2007). In the Central North Sea Basin, adjacent to our study area, Kender et al. (2012) found evidence for an increase in river runoff related to higher regional precipitation over NW Europe at the onset and within the earliest CIE, based on elevated C/N ratios, increase in the abundance of kaolinite clays, and a dinoflagellate community shift indicative of elevated nutrient levels and reduced salinity conditions. An intensification of the hydrological cycle during the PETM is also evident from the relative increases in kaolinite clays at many PETM marginal sites (e.g. Schmitz and Pujalte, 2003; Crouch et al., 2003; Schulte et al., 2013, Robert and Kennett, 1994; Bolle and Adatte, 2001). These deposits are, however, mostly interpreted as the redeposition of older clays during episodes of strongly seasonal precipitation (e.g. Schmitz et al., 2001; Schmitz and Pujalte, 2003). In fact, palaeosoil data from northern Spain (Schmitz and Pujalte, 2003) and terrestrial *n*-alkane δD records from eastern Tanzania (Handley et al., 2012) point to more arid annual conditions in the subtropics during the PETM. This is consistent with model predictions that warmer atmospheric temperatures will cause a stronger latitudinal evaporation-precipitation gradient, with higher evaporation rates in the sub-tropics and higher precipitation rates in mid- and high-latitudes (Manabe, 1996). Consequently, there is a strong regional difference in humidity variations and it is therefore unlikely that a change

in relative humidity as a single factor can account for the consistent difference in the CIE between marine and terrestrial carbon reservoirs observed globally.

Alternatively, it has been suggested that a larger input of angiosperms with respect to gymnosperms during the PETM may overestimate the CIE by up to ~3‰ as angiosperms are more ^{13}C-depleted compared to gymnosperms and also show a larger CIE (Schouten et al., 2007b; Smith et al., 2007). Shifts from gymnosperm- to angiosperm-dominated plant communities have been observed in the Bighorn Basin, Wyoming (Smith et al., 2007) and at the Lomonosov Ridge in the Central Arctic Basin (Sluijs et al., 2006; Schouten et al., 2007b). Kender et al. (2012) studied the pollen and spore assemblages in sediments from the Central North Sea Basin, which also indicated a significant shift in the composition of regional vegetation. At the onset of the PETM, they observed a large decrease in gymnosperm taxa, mainly consisting of coastal swamp conifers and pines, which was replaced by angiosperm taxa, ferns and mosses, indicative of a bog type plant environment. Similar vegetation changes were recently also reported for the Store Bælt section in the eastern North Sea Basin (Willumsen et al., 2013). It is therefore likely that the observed offset in magnitude between the CIEs recorded in the terrestrial-derived *n*-alkanes and marine-derived crenarchaeol at the Store Bælt and Fur sections is mainly driven by regional vegetation changes, although we cannot exclude that an increase in relative humidity also contributed to the larger *n*-alkane CIE.

4.2 Stratification and photic zone anoxia

The low organic carbon content, the ample evidence of bioturbation in the sediments, and the high glauconitic content in the clayey and sandy silt deposits just before the onset of the PETM (Nielsen et al., 1986), are all indicative of a well-oxygenated water column prior to the PETM. Both Danish sections show an abrupt lithological transition at the Palaeocene/Eocene

boundary. The relative amount of organic carbon increases rapidly in concert with the CIE and remains high throughout the PETM interval (Figs. 3a and b). Together with the fine-laminated clays devoid of benthos and high sulfur (pyrite) content, this implies the development of anoxic and sulfidic bottom waters (Nielsen et al., 1986; Pedersen, 1981). This is in agreement with the findings of Kender et al. (2012), suggesting a large scale stratification of the North Sea Basin during the PETM based on palynological and sedimentological evidence.

Supporting evidence for euxinic conditions during the PETM comes from the presence of sulfur-bound isorenieratane at both Danish sections. Sulfur-bound isorenieratane is a diagenetic product of isorenieratene, a characteristic pigment of photosynthetic green sulfur bacteria; besides light (Overmann et al., 1992), these bacteria require free sulfide (H_2S) and anoxic conditions to thrive (Sinninghe Damsté et al., 1993; Summons and Powell, 1986). The presence of these lipids in the Danish PETM sediments, therefore, unambiguously indicates the occurrence of photic zone euxinia (PZE). At the Fur section, sulfur-bound isorenieratane was detected in the entire PETM interval with the highest abundance (~17 μg g^{-1} TOC) occurring 2.51 m after the onset of the CIE (Fig. 3a). Outside the PETM interval this biomarker is below detection limit. In the Store Bælt section sulfur-bound isorenieratane is also detected, although not at all depths within the PETM interval, and the highest abundance (~6 μg g^{-1} TOC) is recorded after the onset of the PETM (Fig. 3b). The evidence for PZE at these two locations suggests that a large part of the eastern North Sea Basin became stratified and had euxinic waters reaching into the photic zone. The development of photic zone euxinia in the North Sea Basin may have multiple causes, such as substantial increases in primary productivity, possibly due to higher nutrient loads by adjacent rivers (Knox, 1996b), and/or oxygen-depletion of intermediate waters due to enhanced microbial recycling and lower solubility of oxygen in warmer waters (Chun et al., 2010; Nicolo et al., 2010). Furthermore,

there has likely been a limited exchange with adjacent water masses, potentially linked with regional tectonic uplift (Bice and Marotzke, 2002; Knox, 1998; Tripati and Elderfield, 2005).

Episodes of photic zone euxinia, coincident with bottom water anoxia, and increased sedimentary organic matter contents have also been reported for the Arctic Ocean, which was a restricted basin during the PETM (Sluijs et al., 2006). The increase in fresh water input due to an enhanced hydrological cycle (Pagani et al., 2006), in combination with an increase in primary productivity, has been invoked to explain the stagnant water masses in this enclosed high latitude basin. A similar supposition has been raised for the North Sea Basin (Kender et al., 2012), based on the influx of fresh-water tolerant dinoflagellate cysts and indications of increased precipitation, suggesting enhanced fluvial runoff. The fact that two restricted basins at different latitudes became anoxic, as well as some coastal sites, suggests that restricted water column ventilation may have been a common feature during the PETM (Sluijs et al., 2014 and references cited therein).

Such a widespread anoxia in shelf seas is reminiscent of the black shale deposits of the early Toarcian. During this period biomarkers of green sulfur bacteria have also been found (Schouten et al., 2000; Sinninghe Damsté and Schouten, 2006; van Breugel et al., 2006), suggesting the development of photic zone euxinia over large areas in the European epicontinental seas and Tethys continental margin. This suggests that the stratification of epicontinental seas may have been a common phenomenon in a greenhouse climate mode (cf. Jenkyns, 2010). Furthermore, a prominent negative carbon isotope excursion is also measured in both inorganic and organic carbon during the early Toarcian (Jenkyns and Clayton, 1997; Jiménez et al., 1996; Kemp et al., 2005). The parallels between the early Toarcian black shales and several PETM sites, therefore, suggest that some of the underlying mechanisms may have been similar. The potentially globally enhanced stratification during the PETM, possibly in combination with elevated productivity, could thus have led to enhanced carbon

burial providing a negative feedback to the release of carbon during the PETM (Bowen and Zachos, 2010).

4.3 Sea surface and air temperature records

For both Danish sections, the TEX_{86} record shows a marked increase parallel to the negative excursion in $\delta^{13}C_{TOC}$, suggesting warmer conditions for the PETM (Figs. 3 and 4). For the Fur section TEX_{86} values decrease during the latest Palaeocene before they rapidly increase across the onset of the PETM to above 0.7 (Fig. 4a). The record of the Store Bælt section exhibits large scatter for the Late Palaeocene; TEX_{86} values average around 0.5 (Fig. 4b). A decrease in TEX_{86} is recorded just before the onset of the PETM, just as for the Fur record. Overall, TEX_{86} values during the PETM are slightly lower at the Store Bælt section than those recorded at the Fur section (Figs. 4a and b).

We applied the TEX_{86}^{H} calibration of Kim et al. (2010) to convert the TEX_{86} into SSTs. This calibration is recommended for palaeothermometry of greenhouse worlds with SST >15 °C. The decreasing trend in TEX_{86} values for the latest Palaeocene for the Fur section corresponds to a temperature decrease from 24 to 17 °C (Fig. 4a). This is followed by a sharp increase at the onset of the PETM towards a maximum SST of ~31 °C (Fig. 4a). For the Store Bælt section, Late Palaeocene SSTs ranged between 28 and 16 °C, and although the record is subjected to considerable scatter, low SST values are also recorded at this site just before the onset of the PETM (Fig. 4b). Across the onset, SST increases to a maximum of ca. 30 °C followed by a gradual decrease during the course of the PETM. These peak SST estimates are within the range of peak estimates obtained for the mid-latitude New Jersey shelf (Zachos et al., 2006; Sluijs et al., 2007b). Application of the TEX_{86}^{L} and $1/TEX_{86}$ calibrations yield overall lower absolute temperatures in comparison with TEX_{86}^{H} SSTs, while application of the

Baysian calibration of Tierney and Tingley (2014) yielded somewhat different absolute temperatures, but all the records do show the same trends (data not shown).

Most PETM sections show either relatively stable background SST values (Sluijs et al., 2011; Zachos et al., 2003), or even a warming that preceded the negative CIE (Sluijs et al., 2007b; Tripati and Elderfield, 2004). However, both Danish sections exhibit a large decrease in SST of ca. 7 °C just prior to the onset of the CIE in the glauconitic silt unit. It is possible that the TEX_{86} records at our sites are biased for this time-interval. For instance, the TEX_{86} values can be affected by the input of soil-derived isoprenoid GDGTs which can be assessed by the BIT index (Weijers et al., 2006). Before the PETM, BIT values are generally high between 0.3 to 0.7 for both sections (Figs. 4a and b). These high values indicate that the TEX_{86} values may indeed be affected by soil organic matter input and thus the SST estimates for the latest Palaeocene may be biased. Just before the onset of the CIE in the glauconitic silt unit, BIT values gradually decrease to <0.1 and remain low during the PETM (Figs. 4a and b), suggesting that TEX_{86} values are unlikely to be substantially affected by terrestrial input for this part of the section. The reason for the high BIT values and the variability in TEX_{86} values may be that the GDGT distributions are affected by oxic degradation. The TOC values for the Late Palaeocene part of both sections are low (<0.6 %; Figs. 3a and b) and the depositional environment was oxic prior to the PETM (see also section 4.2), and thus organic matter, including GDGTs, were substantially exposed to oxygen. This is supported by palynological observations of organic particles in the Holmehus Formation, which are severely degraded and corroded (Heilmann-Clausen et al, 1985). Indeed, before the PETM, concentrations of the branched GDGTs and crenarchaeol are low (<0.01 μg g^{-1} sediment; Fig. 4b). Concomitant with the onset of the CIE, and higher TOC values, there is a substantial increase in the concentration of crenarchaeol towards peak values of ~0.6 μg g^{-1} sediment (Fig. 4b). In contrast, the branched GDGT concentration during that same interval increases considerably

less (up to ~0.03 μg g^{-1} sediment; Fig. 4b). This is in agreement with the findings of Huguet et al. (2009) and Lengger et al. (2013), who showed that upon prolonged exposure to oxic conditions, crenarchaeol is more prone to oxic degradation during early diagenesis than branched GDGTs, leading to higher BIT values. Thus, the high BIT values prior to the PETM may have been caused by severe oxic degradation. By association, this selective degradation of the marine signal compared to the terrestrial signal may have also biased TEX_{86} temperature estimates, because soil organic matter contain isoprenoid GDGTs with a different distribution than marine isoprenoid GDGTs. However, it is still uncertain to what degree it affects the temperature estimates (Huguet et al., 2009). Finally, the GDGTs may have been derived from sources other than Thaumarchaeota which are thought to be the primary source for marine GDGTs. Analysis of the $\delta^{13}C$ values of the biphytane moieties of GDGTs at the Fur and Store Bælt sections showed that acyclic and monocyclic biphytanes exhibited relatively depleted ^{13}C values (down to -31 ‰) compared to the tricyclic biphytane derived from crenarchaeol (ca. -21‰; Schoon et al., 2013). This suggests that some of the GDGTs, in particular GDGT-1, may partly derive from Archaea associated with methane cycling (Schoon et al., 2013). Thus, a larger input of this GDGT to the sediments deposited just before the onset of the CIE in the glauconitic silt unit may have caused an underestimation of the SSTs in this interval.

If the TEX_{86} values from the glauconitic silt unit with the unusual cooling are excluded and we average the remaining pre-PETM TEX_{86} values (23 ± 4 °C for Store Bælt, and 24 °C for Fur), we obtain an average temperature increase of ~7°C across the Palaeocene-Eocene boundary for both Danish sections. Application of TEX_{86}^{L} or $1/TEX_{86}$ calibrations yield an identical increase of ~7°C, while the Bayesian calibration model of Tierney and Tingley (2014) yielded an increase of 11-12 °C. A 7 °C warming of the North Sea surface waters is consistent with the mid-latitude temperature records from the New Jersey shelf based on the

$\delta^{18}O$ in planktonic foraminifera and TEX_{86} (Sluijs et al., 2007b; Zachos et al., 2006; John et al., 2008) as well as in the southern hemisphere at the East Tasman Plateau (Sluijs et al., 2011) and the mid-Waipara section, New Zealand (Hollis et al., 2012; see also Fig. 1). As previously suggested by Zachos et al. (2006), it is possible that shallow marine sites are affected by variations in regional and seasonal parameters, causing a larger warming at continental margins in comparison with open marine waters.

Interestingly, reconstructed MATs based on the MBT'/CBT proxy for the Fur section show a similar pattern as the TEX_{86} record: a temperature decrease from 19 to 16 °C for the latest Palaeocene followed by an increase of 4 °C across the Palaeocene-Eocene boundary (Fig. 4a). Peak MAT values (~24 °C) are reached at the same depth as peak SST values (2.51 m; Fig. 4b), resulting in an overall increase of MAT of 5-8 °C. The similar patterns between the SST and MAT records suggests that potential biases on the TEX_{86} temperature record prior to the PETM, as discussed above, may have not been severe. In contrast to the Fur section and the TEX_{86} record, the MBT'/CBT record of the Store Bælt section exhibits no warming trend and MAT estimates remain similar across the onset of the PETM (Fig. 4b). Peak MAT values (~20 °C) are lower than those recorded for the Fur section and occur between 129.75 and 128.45 mcd. As discussed above, the Store Bælt section was likely further removed from land than the Fur section and did not receive a large influx of soil-derived organic matter, which may explain why at this location the MBT'/CBT does not show any warming trend. The only other available MBT'/CBT record of the PETM is from the Arctic continent. Absolute temperature values are lower as would be expected for this higher latitude site, from ~15 °C for the Late Palaeocene towards ~21 °C during the PETM (Peterse et al., 2012, recalculated from Weijers et al., 2007a). This corresponds to a ~6 ºC warming of the continents around the Arctic region, which is in good agreement with the MBT'/CBT record of the Fur section.

5. Conclusions

We studied two PETM sections from the eastern part of the North Sea Basin. Both Danish sections are marked by a negative CIE in TOC of 5-6 ‰. Analyses of the stable carbon isotopes of higher plant-derived long-chain *n*-alkanes reveal a terrestrial CIE of 4-6 ‰ at Store Bælt, but at Fur the terrestrial CIE magnitude is 1-2 ‰ higher and seems to precede the CIE in TOC. The differences in the distribution patterns and $\delta^{13}C$ profiles of the *n*-alkanes between the two sites, likely reflect regional rather than global changes. The terrestrial CIE is larger than reconstructed for the marine CIE, probably due to a change in vegetation.

The onset of the CIE is accompanied by a marked change in lithology, increasing organic matter content and the presence of sulfur-bound isorenieratane, indicating a substantial change in depositional environment from well-oxygenated to anoxic and sulfidic, likely due to a combination of diminished oxygen supply by intermediate waters, increased primary productivity and an increase in fluvial runoff. These euxinic conditions are similar to those previously reported for the Lomonosov Ridge in the Arctic Ocean, suggesting that restricted water column ventilation was common in semi-enclosed basins during the PETM.

The TEX_{86} SST records show a warming of ~7 °C during the PETM. This warming is preceded by a remarkable cooling of several degrees prior to the onset of the PETM, potentially caused by oxic degradation and selective preservation of soil organic matter during the latest Palaeocene, or by the additional input of GDGTs from sources other than Thaumarchaeota. Continental air temperatures reconstructed using the MBT'/CBT index show a remarkable similar trend, including a cooling prior to the PETM at the Fur section, but not at the Store Bælt section. It is possible that these temperature records reflect additional local climate changes besides the global changes associated with the PETM. Our study thus

suggests that it is important to study climate records from multiple locations within a region to separate regional from global climate variability.

Acknowledgments

We thank Dr. Simon George, Dr. Ann Pearson and three anonymous reviewers for their constructive comments on the manuscript. We thank Marianne Baas, Jort Ossebaar, Anchelique Mets, Michiel Kienhuis and Daphne Rekers for their laboratory assistance. We thank Katarzyna Śliwińska and Pi Suhr Willumsen for useful discussions. Financial support for this research was provided by the Darwin Center for Biogeosciences and a VICI grant from the Netherlands Organisation for Scientific Research to SS.

References

Berg, I.A., Kockelkorn, D., Buckel, W., Fuchs, G., 2007. A 3-hydroxypropionate/4-hydroxybutyrate autotrophic carbon dioxide assimilation pathway in archaea. Science 318, 1782-1786.

Bijl, P.K., Schouten, S., Sluijs, A., Reichart, G.-J., Zachos, J.C., Brinkhuis, H., 2009. Early Palaeogene temperature evolution of the southwest Pacific Ocean. Nature 461, 776-779.

Bøggild, O.B., 1918. Den vulkanske aske i moleret. Danmarks Geologiske Undersøgelse II Række, No. 33, 1-159.

Bolle, M.P., Adatte, T., 2001. Palaeocene early Eeocene climatic evolution in the Tethyan realm: clay mineral evidence. Clay Minerals 36, 249-261.

Bolle, M.-P., Pardo, A., Hinrichs, K.-U., Adatte, T., Von Salis, K., Keller, G., Muzylev, N., 2000. The Paleocene-Eocene transition in the marginal northeastern Tethys (Kazakhstan and Uzbekistan). International Journal Earth Sciences 89, 390-414.

Bottjer, D.J., Droser, M.L., 1992. Paleoenvironmental patterns of biogenic sedimentary structures. In: Maples, C.G. and West, R.R. (Eds.), Trace Fossils, Paleontological Society Short Courses in Paleontology No. 5, 130-144. University of Tenessee, Knoxville, UTK publication EO1-1040-003-93.

Bowen, G.J., Beerling, D.J., Koch, P.L., Zachos, J.C., Quattlebaum, T., 2004. A humid climate state during the Palaeocene/Eocene thermal maximum. Nature 432, 495-499.

Bowen, G.J., Zachos, J.C., 2010. Rapid carbon sequestration at the termination of the Palaeocene-Eocene Thermal Maximum. Nature Geoscience 3, 866-869.

Bray, E.E., Evans, E.D., 1961. Distribution of *n*-paraffins as a clue to recognition of source beds. Geochimica et Cosmochimica Acta, 22, 2-15.

Caballero, R., Huber, M, 2013. State-dependent climate sensitivity in past warm climates and its implications for future climate projections. Proceedings of the National Academy of Sciences 110, 14162–14167.

Chun, C.O.J., Delaney, M.L., Zachos, J.C., 2010. Paleoredox changes across the Paleocene-Eocene thermal maximum, Walvis Ridge (ODP Sites 1262, 1263, and 1266): Evidence from Mn and U enrichment factors. Paleoceanography 25, PA4202, 1-13.

Crouch, E.M., Dickens, G.R., Brinkhuis, H., Aubry, M.P., Hollis, C.J., Rogers, K.M., Visscher, H., 2003. The *Apectodinium* acme and terrestrial discharge during the Paleocene-Eocene thermal maximum: new palynological, geochemical and calcareous nannoplankton observations at Tawanui, New Zealand. Palaeogeography, Palaeoclimatology, Palaeoecology 194, 387-403.

Dickens, G.R., 2011. Down the Rabbit Hole: toward appropriate discussion of methane release from gas hydrate systems during the Paleocene-Eocene thermal maximum and other past hyperthermal events. Climate of the Past 7, 831-846.

Diefendorf, A.F., Mueller, K.E., Wing, S.L., Koch, P.L., Freeman, K.H., 2010. Global patterns in leaf ^{13}C discrimination and implications for studies of past and future climate. Proceedings of the National Academy of Sciences USA 107, 5738-5743.

Eglinton, G., Hamilton, R.J., 1967. Leaf epicuticular waxes. Science 156, 1322-1335.

Han, J. & Calvin, M., 1969. Hydrocarbon distribution of algae and bacteria, and microbiological activity in sediments. Proceedings of the National Academy of Sciences USA 64, 436-443.

Handley, L., Pearson, P.N., McMillan, I.K., Pancost, R.D., 2008. Large terrestrial and marine carbon and hydrogen isotope excursions in a new Paleocene/Eocene boundary section from Tanzania. Earth and Planetary Science Letters 275, 17-25.

Handley, L., Crouch, E.M., Pancost, R.D. 2011. A New Zealand record of sea level rise and environmental change during the Paleocene–Eocene Thermal Maximum. Palaeogeography, Palaeoclimatology, Palaeoecology 305, 185-200.

Heilmann-Clausen, C., 1994. Review of Paleocene dinoflagellates from the North Sea region Geologiska Föreningen Förhandlingar 116, 51-53.

Heilmann-Clausen, C. 1995. Palæogene aflejringer over Danskekalken. In: Nielsen. O.B. (ed.), Aarhus Geokompendier No. 1, Danmarks geologi fra Kridt til i dag, 69-114.

Heilmann-Clausen, C., 2006. Koralrev og lerhav (excl. Danian). In: G. Larsen (Ed.), Naturen i Danmark, Geologien. Gyldendal, Copenhagen, 181-186 & 191-226.

Heilmann-Clausen, C., 2014. Possible varves in the PETM interval in Denmark. Rendiconti Online della Societa Geologia Italia. 31, 97-98.

Heilmann-Clausen, C., Schmitz, B., 2000. The late Paleocene thermal maximum $\delta^{13}C$ excursion in Denmark? Gff 122, 70.

Heilmann-Clausen, C., Nielsen, O.B., Gersner, F. 1985. Lithostratigraphy and depositional environments in the Upper Paleocene and Eocene of Denmark. Bulletin of the Geological Society of Denmark 33, 287-323.

Hilgen, F.J., Kuiper, K.F., Lourens, L.J., 2010. Evaluation of the astronomical time scale for the Paleocene and earliest Eocene. Earth and Planetary Science Letters. 300, 139-151.

Hollis, C.J., Taylor, K.W.R., Handley, L., Pancost, R.D., Huber, M., Creech, J.B., Hines, B.R., Crouch, E.M., Morgans, H.E.G., Crampton, J.S., Gibbs, S., Pearson, P.N., Zachos, J.C., 2012. Early Paleogene temperature history of the Southwest Pacific Ocean: Reconciling proxies and models. Earth and Planetary Science Letters 349-350, 53-66.

Hopmans, E.C., Weijers, J.W.H., Schefuß, E., Herfort, L., Sinninghe Damsté, J.S., Schouten, S., 2004. A novel proxy for terrestrial organic matter in sediments based on branched and isoprenoid tetraether lipids. Earth and Planetary Science Letters 224, 107-116.

Huber, M., Caballero, R., 2011. The early Eocene equable climate problem revisited. Climate of the Past 7, 603-633.

Huguet, C., Kim, J.-H., de Lange, G.J., Sinninghe Damsté, J.S., Schouten, S., 2009. Effects of long term oxic degradation on the $U^{K'}_{37}$, TEX_{86} and BIT organic proxies. Organic Geochemistry 40, 1188-1194.

Jenkyns, H.C., 2010. Geochemistry of oceanic anoxic events. Geochemistry Geophysics Geosystems 11, 1-30.

Jenkyns, H.C., Clayton, C.J., 1997. Lower Jurassic epicontinental carbonates and mudstones from England and Wales: chemostratigraphic signals and the early Toarcian anoxic event. Sedimentology 44, 687-706

Jiménez, A.P., Jimenez de Cisneros, C., Rivas, P.,Vera, J.A., 1996, The early Toarcian anoxic event in the westernmost Tethys (Subbetic): Paleogeographic and paleobiogeographic significance: Journal of Geology 104, 399–416.

John, C.M., Bohaty, S.M., Zachos, J.C., Sluijs, A., Gibbs, S., Brinkhuis, H., Bralower, T.J., 2008. North American continental margin records of the Paleocene-Eocene thermal maximum: Implications for global carbon and hydrological cycling. Paleoceanography 23, PA2217, 1-20.

Kemp, D.B., Coe, A.L., Cohen, A.S., Schwark, L., 2005. Astronomical pacing of methane release in the Early Jurassic period. Nature 437, 396–399.

Kender, S., Stephenson, M.H., Riding, J.B., Leng, M.J., Knox, R, W.O'B., Peck, V.L., Kendrick, C.P., Ellis, M.A., Vane, C.H., Jamieson, R., 2012. Marine and terrestrial environmental changes in NW Europe preceding carbon release at the Paleocene-Eocene transition. Earth and Planetary Science Letters 353-354, 108-120.

Kennett, J.P., Stott, L.D., 1991. Abrupt deep-sea warming, palaeoceanographic changes and benthic extinctions at the end of the Palaeocene. Nature 353, 225-229.

Kim, J.-H., van der Meer, J., Schouten, S., Helmke, P., Willmott, V., Sangiorgi, F., Koc, N., Hopmans, E.C., Sinninghe Damsté, J.S., 2010. New indices and calibrations derived from the distribution of crenarchaeal isoprenoid tetraether lipids: Implications for past sea surface temperature reconstructions. Geochimica et Cosmochimica Acta 74, 4639-4654.

Knox, R.W. O'B., 1996a:Tectonic controls on sequence development in the Paleocene and earliest Eocene of SE England: implications for North Sea stratigraphy, in: Hesselbo, S.P. & Parkinson, D.N. (Eds), Sequence stratigraphy in British geology, Geological Society Special Publication (London) 103, 209-230.

Knox, R.W.O'B., 1996b. Correlation of the Early Paleogene in Northwest Europe: an overview, in: Knox, R.W.O'B., Corfield, R.M. & Dunay, R.E. (Eds.), Correlation of the Early Paleogene in Northwest Europe, Geological Society Special Publication, London, 1–11.

Knox, R. W. O'B., 1998. The tectonic and volcanic history of the North Atlantic region during the Paleocene-Eocene transition: implications for NW European and global biotic events, in: Aubry, A.-P., Lucas, S. and Berggren, W. A. (Eds.), Late Paleocene-Early Eocene Climatic and Biotic Events in the Marine and Terrestrial Records, Columbia University Press, New York, 91–102.

Knox, R.W.O'B, Bosch, J.H.A., Rasmussen, E. S., Heilmann-Clausen, C., Hiss, M., De Lugt, I.R., Kasinski, J., King, C., Köthe, A., Slodkowska, B., Standke, G. & Vandenberghe, N., 2010: Cenozoic. In: Dornenbaal, H. & Stevenson, A. (Eds.), Petroleum Geological Atlas of the Southern Permian Basin Area, EAGE Publications b.v., Houten, 211-223.

Laursen, G.V. and King, C., 1999. Preliminary results of a foraminiferal analysis of a core from Østerrende, Denmark. In: Andreasson, F.P., Schmitz, B., and Thompson, E.I. (Eds.), Early Paleogene warm climates and biosphere dynamics, Abstract Volume. Earth Science Centre Göteburg University, C21.

Lengger S.K., Kraaij M., Baas M., Tjallingii R., Stuut J.-B., Hopmans E.C., Sinninghé Damste J.S., Schouten S., 2013. Differential degradation of intact polar and core glycerol dialkyl glycerol tetraether lipids upon post-depositional oxidation. Organic Geochemistry 65, 83-93.

Liu, Z., Pagani, M., Zinniker, D., DeConto, R., Huber, M., Brinkhuis, H., Shah, S.R., Leckie, R.M., Pearson, A., 2009. Global cooling during the Eocene-Oligocene climate transition. Science 323, 1187-1190.

Manabe, S., Early development in the study of greenhouse warming: The emergence of climate models, Ambio, 26, 47–51, 1996.

Marzi, R., Torkelson, B.E., Olson, R.K., 1993. A revised carbon preference index. Organic Geochemistry 20, 1303-1306.

McInerney, F.A., Wing, S.L., 2011. The Paleocene-Eocene Thermal Maximum: A perturbation of carbon cycle, climate, and biosphere with implications for the future. Annual Reviews in Earth and Planetary Sciences 39, 489-516.

Nicolo, M.J., Dickens, G.R., Hollis, C.J., 2010. South Pacific intermediate water oxygen depletion at the onset of the Paleocene-Eocene thermal maximum as depicted in New Zealand margin sections. Paleoceanography 25, PA4210-1-PA4210-12.

Nielsen, O.B., Baumann, J. Zhang, D., Heilmann-Clausen, C. & Larsen G, 1986. Tertiary Deposits in Store Bælt. In: Møller J.T. (Ed.), Twenty five Years of Geology in Aarhus, Geoskrifter No. 24, 235-253.

Overmann, J., Cypionka, H., Pfennig, N., 1992. An extremely low-light-adapted phototrophic sulfur bacterium from the Black Sea. Limnology and Oceanography 37, 150-155.

Pagani, M., Pedentchouk, N., Huber, M., Sluijs, A., Schouten, S., Brinkhuis, H., Sinninghe Damsté, J.S., Dickens, G.R., the Expedition 302 Scientists, 2006. Arctic hydrology during global warming at the Palaeocene/Eocene thermal maximum. Nature 442, 671-675.

Pagani, M., Huber, M., Liu, Z., Bohaty, S.M., Henderiks, J., Sijp, W., Krishnan, S., DeConto, R.M., 2011. The role of carbon dioxide during the onset of Antarctic glaciation. Science 334, 1261-1264.

Pearson, P.N., Ditchfield, P.W., Singano, J., Harcourt-Brown, K.G., Nicholas, C.J., Olsson, R.K., Shackleton, N.J., Hall, M.A., 2001. Warm tropical sea surface temperatures in the Late Cretaceous and Eocene epoch. Nature 413, 481-487.

Pedersen, G.K., 1981. Anoxic events during sedimentation of a Palaeogene diatomite in Denmark. Sedimentology 28, 487-504.

Pedersen, G.K., Surlyk, F., 1983. The Fur Formation, a late Paleocene ash-bearing diatomite from northern Denmark. Bulletin of the Geological Society of Denmark 32, 43-65.

Pedersen, G.K., Pedersen, S.A.S., Steffensen, J., Pedersen, C.S., 2004. Clay content of a clayey diatomite, the Early Eocene Fur Formation, Denmark. Bulletin of the Geological Society of Denmark 51, 159-177.

Peterse, F., Kim, J.H., Schouten, S., Kristensen, D.K., Koç, N., Sinninghe Damsté, J.S., 2009. Constraints on the application of the MBT/CBT palaeothermometer at high latitude environments (Svalbard, Norway). Organic Geochemistry 40, 692-699.

Peterse, F., van der Meer, J. Schouten, S., Weijers, J.W.H., Fierer, N, Jackson, R.B., Kim J-H., Sinninghe Damsté, J.S., 2012. Revised calibration of the MBT–CBT paleotemperature proxy based on branched tetraether membrane lipids in surface soils. Geochimica et Cosmochimica Acta 96, 215-229.

Robert, C., Kennett, J.P., 1994. Antarctic subtropical humid episode at the Paleocene-Eocene boundary – clay-mineral evidence. Geology 22, 211-214.

Schmitz, B., Pujalte, V., 2003. Sea-level, humidity, and land-erosion records across the initial Eocene thermal maximum from a continental-marine transect in northern Spain. Geology 31, 689-692.

Schmitz, B., Peucker-Ehrenbrink, B., Heilmann-Clausen, C., Åberg, G., Asaro, F., Lee, C.-T.A., 2004. Basaltic explosive volcanism, but no comet impact, at the Paleocene-Eocene boundary: high-resolution chemical and isotopic records from Egypt, Spain and Denmark. Earth and Planetary Science Letters 225, 1-17.

Schoon, P.L., Sluijs, A., Sinninghe Damsté, J.S., Schouten, S., 2011. Stable carbon isotope patterns of marine biomarker lipids in the Arctic Ocean during Eocene Thermal Maximum 2. Paleoceanography 26, PA3215-1-PA3215-15.

Schoon, P.L., Heilmann-Clausen, C., Schultz, B.P., Sluijs, A., Sinninghe Damsté, J.S., Schouten, S., 2013. Recognition of Early Eocene global carbon isotope excursions using lipids of marine Thaumarchaeota. Earth and Planetary Science Letters 373, 160-168.

Schouten, S., van Kaam-Peters, H.M.E., Rijpstra, W.I.C., Schoell, M., Sinninghe Damsté, J.S., 2000. Effects of an oceanic anoxic event on the stable carbon isotopic composition of Early Toarcian carbon. American Journal of Science 300, 1-22.

Schouten, S., Hopmans, E.C., Schefuß, E., Sinninghe Damsté, J.S., 2002. Distributional variations in marine crenarchaeotal membrane lipids: a new tool for reconstructing ancient sea water temperatures? Earth and Planetary Science Letters 204, 265-274.

Schouten, S., Huguet, C., Hopmans, E.C., Kienhuis, M.V.M., Sinninghe Damsté, J.S., 2007a. Analytical methodology for TEX_{86} paleothermometry by high-performance liquid chromatography/atmospheric pressure chemical ionization-mass spectrometry. Analytical Chemistry 79, 2940-2944.

Schouten, S., Woltering, M., Rijpstra, W.I.C., Sluijs, A., Brinkhuis, H., Sinninghe Damsté, J.S., 2007b. The Paleocene-Eocene carbon isotope excursion in higher plant organic matter: Differential fractionation of angiosperms and conifers in the Arctic. Earth and Planetary Science Letters 258, 581-592.

Schrag, D.P., 1999. Effects of diagenesis on the isotopic record of late paleogene tropical sea surface temperatures. Chemica Geology 161, 215-224.

Schulte, P., Schwark, L., Stassen, P., Kouwenhoven, T.J., Bornemann, A., Speijer, R.P., 2013. Black shale formation during the Latest Danian Event and the Paleocene-Eocene Thermal Maximum in central Egypt: Two of a kind? Palaeogeography, Palaeoclimatology, Palaeoecology 371, 9-25.

Sinninghe Damsté, J.S., Wakeham, S.G., Kohnen, M.E.L., Hayes, J.M., de Leeuw, J.W., 1993. A 6,000 year sedimentary molecular record of chemocline excursions in the Black Sea. Nature 362, 827-829.

Sinninghe Damsté, J.S., Köster, J., 1998. A euxinic southern North Atlantic Ocean during the Cenomanian/Turonian oceanic anoxic event. Earth and Planetary Science Letters 158, 165-173.

Sinninghe Damsté, J.S., Schouten, S., 2006. Biological markers for anoxia in the photic zone of the water column. In: The Handbook of Environmental Chemistry. Springer-Verlag, Berlin, Heidelberg, pp. 128-163.

Sluijs, A., Dickens, G.R., 2012. Assessing offsets between the $\delta^{13}C$ of sedimentary components and the global exogenic carbon pool across early Paleogene carbon cycle perturbations. Global Biogeochemical Cycles 26, doi:10.1029/2011GB004224.

Sluijs, A., Schouten, S., Pagani, M., Woltering, M., Brinkhuis, H., Sinninghe Damsté, J.S., Dickens, G.R., Huber, M., Reichart, G.-J., Stein, R., Matthiesen, J., Lourens, L.J., Pedentchouk, N., Backman, J., Moran, K., the Expedition 302 Scientists, 2006. Subtropical Arctic Ocean temperatures during the Palaeocene/Eocene thermal maximum. Nature 441, 610-612.

Sluijs, A., Bowen, G.J., Brinkhuis, H., Lourens, L.J., Thomas, E., 2007a. The Palaeocene-Eocene Thermal Maximum super greenhouse: biotic and geochemical signatures, age models and mechanisms of global change. In: Deep-Time perspectives on climate change: Marrying the signal from computer models and biological proxies. The Geological Society, London, pp. 323-349.

Sluijs, A., Brinkhuis, H., Schouten, S., Bohaty, S.M., John, C.M., Zachos, J.C., Reichart, G.-J., Sinninghe Damsté, J.S., Crouch, E.M., Dickens, G.R., 2007b. Environmental precursors to rapid light carbon injection at the Palaeocene/Eocene boundary. Nature 450, 1218-12U5.

Sluijs, A., Röhl, U., Schouten, S., Brumsack, H.J., Sangiorgi, F., Sinninghe Damsté, J.S., Brinkhuis, H., 2008. Arctic late Paleocene-early Eocene paleoenvironments with special

emphasis on the Paleocene-Eocene thermal maximum (Lomonosov Ridge, Integrated Ocean Drilling Program Expedition 302). Paleoceanography 23, PA1S11.

Sluijs, A., Bijl, P.K., Schouten, S., Röhl, U., Reichart, G.-J., Brinkhuis, H., 2011. Southern ocean warming, sea level and hydrological change during the Paleocene-Eocene thermal maximum. Climate of the Past 7, 47-61.

Sluijs, A., van Roij, L., Harrington, G.J., Schouten, S., Sessa, J.A., LeVay, L.J., Reichart, G.J. Slomp C.P., 2014. Extreme warming, photic zone euxinia and sea level rise during the Paleocene/Eocene Thermal Maximum on the Gulf of Mexico Coastal Plain; connecting marginal marine biotic signals, nutrient cycling and ocean deoxygenation. Climate of the Past 10, 1421-1439.

Smith, F.A., Wing, S.L., Freeman, K.H., 2007. Magnitude of the carbon isotope excursion at the Paleocene-Eocene thermal maximum: The role of plant community change. Earth and Planetary Science Letters 262, 50-65.

Stap, L., Sluijs, A., Thomas, E., Lourens, L., 2009. Patterns and magnitude of deep sea carbonate dissolution during Eocene Thermal Maximum 2 and H2, Walvis Ridge, southeastern Atlantic Ocean. Paleoceanography 24, PA1211, 1-13.

Storey, M., Duncan, R.A., Swisher III, C.C., 2007. Paleocene-Eocene thermal maximum and the opening of the northeast Atlantic. Science 316, 587-589.

Summons, R.E., Powell, T.G., 1986. *Chlorobiaceae* in Palaeozoic seas revealed by biological markers, isotopes and geology. Nature 319, 763-765.

Thomas, D.J., Zachos, J.C., Bralower, T.J., Thomas, E., Bohaty, S., 2002. Warming the fuel for the fire: Evidence for the thermal dissociation of methane hydrate during the Paleocene-Eocene thermal maximum. Geology 30, 1067-1070.

Tierney J. E., Tingley M. P., 2014. A Bayesian, spatially-varying calibration model for the TEX_{86} proxy. Geochimica et Cosmochimica Acta 127, 83–106.

Tripati, A.K., Elderfield, H., 2004. Abrupt hydrographic changes in the equatorial Pacific and subtropical Atlantic from foraminiferal Mg/Ca indicate greenhouse origin for the thermal maximum at the Paleocene-Eocene Boundary. Geochemistry Geophysics Geosystems 5 (2), doi:10.1029/2003GC000631-11.

Tripati, A.K., Elderfield, H., 2005. Deep-sea temperature and circulation changes at the Paleocene-Eocene thermal maximum. Science 308, 1894-1898.

Uchikawa, J., Zeebe, R.E., 2010. Examining possible effects of seawater pH decline on foraminiferal stable isotopes during the Paleocene-Eocene Thermal Maximum. Paleoceanography 25, PA2216-1-PA2216-14.

van Breugel, Y., Baas, M., Schouten, S., Mattioli, E., Sinninghe Damsté, J.S., 2006. Isorenieratane record in black shales from the Paris Basin, France: Constraints on recycling of respired CO_2 as a mechanism for negative carbon isotope shifts during the Toarcian oceanic anoxic event. Paleoceanography 21, PA4220-1-PA4220-8.

Weijers, J.W.H., Schouten, S., Spaargaren, O.C., Sinninghe Damsté, J.S., 2006. Occurrence and distribution of tetraether membrane lipids in soils: Implications for the use of the TEX_{86} proxy and the BIT index. Organic Geochemistry 37, 1680-1693.

Weijers, J.W.H., Schouten, S., Sluijs, A., Brinkhuis, H., Sinninghe Damsté, J.S., 2007a. Warm arctic continents during the Palaeocene-Eocene thermal maximum. Earth and Planetary Science Letters 261, 230-238.

Weijers, J.W.H., Schouten, S., van den Donker, J.C., Hopmans, E.C., Sinninghe Damsté, J.S., 2007b. Environmental controls on bacterial tetraether membrane lipid distribution in soils. Geochimica et Cosmochimica Acta 71, 703-713.

Westerhold, T., Röhl, U., McCarren, H.K., Zachos, J.C., 2009. Latest on the absolute age of the Paleocene-Eocene Thermal Maximum (PETM): New insights from exact stratigraphic position of key ash layers +19 and -17. Earth and Planetary Science Letters 287, 412-419.

Willumsen, P.S., Schultz, B.P., Sylvestersen, R., 2013. Rapid warming at the PETM and its influence on vegetation in Denmark. 1st International Congress on Stratigraphy (STRATI 2013)

Wing, S.L., Harrington, G.J., Smith, F.A., Bloch, J.I., Boyer, D.M., Freeman, K.H., 2005. Transient floral change and rapid global warming at the paleocene-eocene boundary. Science 310, 993-996.

Zachos, J.C., Wara, M.W., Bohaty, S., Delaney, M.L., Petrizzo, M.R., Brill, A., Bralower, T.J., Premoli-Silva, I., 2003. A transient rise in tropical sea surface temperature during the Paleocene-Eocene Thermal Maximum. Science 302, 1551-1554.

Zachos, J.C., Röhl, U., Schellenberg, S.A., Sluijs, A., Hodell, D.A., Kelly, D.C., Thomas, E., Nicolo, M., Raffi, I., Lourens, L.J., McCarren, H., Kroon, D., 2005. Rapid acidification of the ocean during the Paleocene-Eocene thermal maximum. Science 308, 1611-1615.

Zachos, J.C., Schouten, S., Bohaty, S., Quattlebaum, T., Sluijs, A., Brinkhuis, H., Gibbs, S.J., Bralower, T.J., 2006. Extreme warming of mid-latitude coastal ocean during the Paleocene-Eocene Thermal Maximum: Inferences from TEX_{86} and isotope data. Geology 34, 737-740.

Zeebe, R.E., Zachos, J.C., 2007. Reversed deep-sea carbonate ion basin gradient during Paleocene-Eocene thermal maximum. Paleoceanography 22, PA3201-1-PA3201-17.

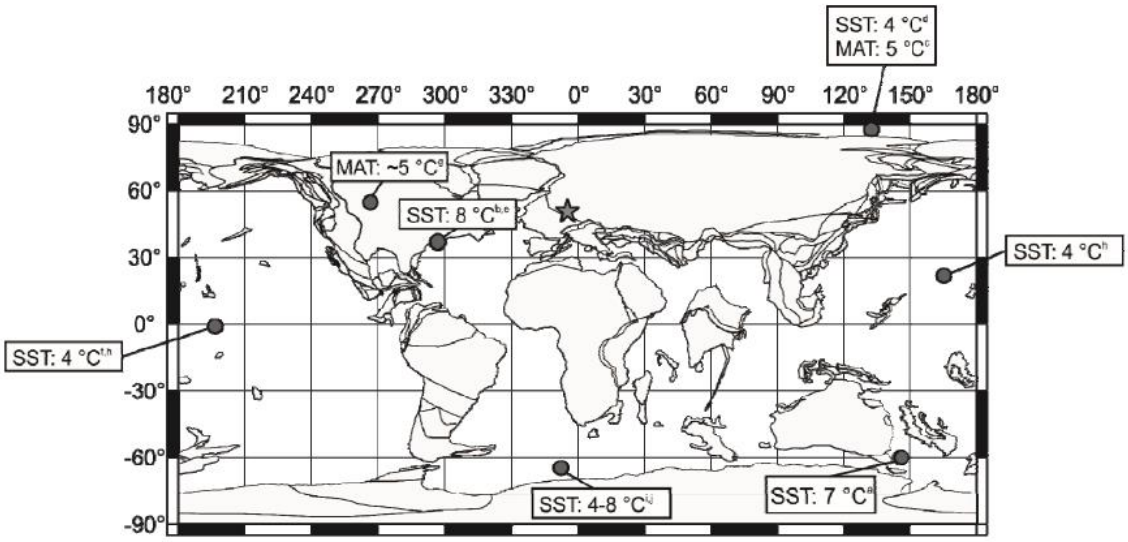

Figure 1: Plate tectonic reconstruction of 55 Ma (www.odsn.de/odsn) and reconstructed warming during the PETM. The dots show locations where PETM SST and MAT warming have been reconstructed: [a]Hollis et al., 2012 ($pTEX_{86}$), [b]Sluijs et al., 2011 (TEX_{86}), [c]Sluijs et al., 2007b (TEX_{86}), [d]Peterse et al., 2012, recalculated from Weijers et al., 2007a (MBT/CBT), [e]Sluijs et al., 2006 (TEX_{86}), [f]Zachos et al., 2006 (TEX_{86}), [g]Tripati and Elderfield, 2005 (Mg/Ca and $\delta^{18}O$ of planktonic foraminifera), [h]Wing et al., 2005 (leaf margin analysis), [i]Zachos et al., 2003 (Mg/Ca and $\delta^{18}O$ of planktonic foraminifera), [j]Thomas et al. 2002 ($\delta^{18}O$ of planktonic foraminifera), [k]Kennett and Stott, 1991 ($\delta^{18}O$ of planktonic foraminifera). The star indicates the location of this study.

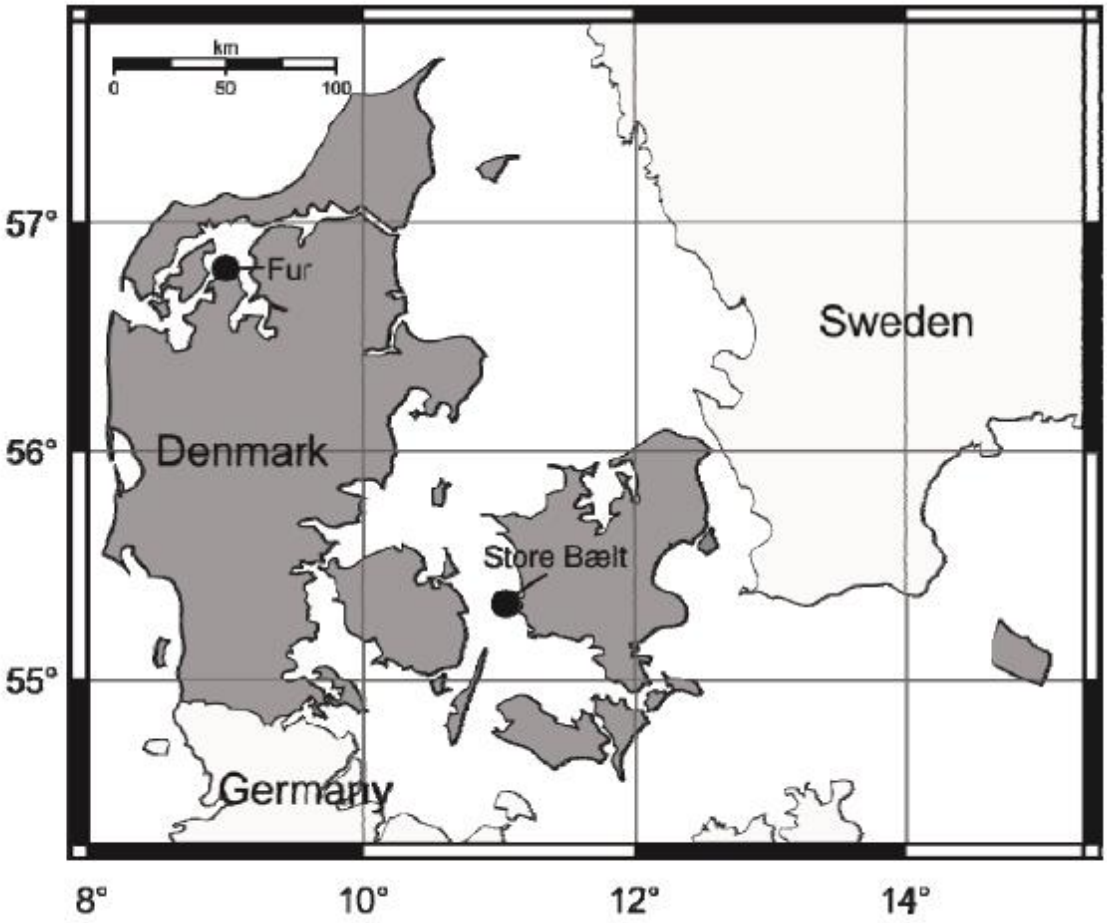

Figure 2: Map of Denmark showing the location of the two study sites at Fur Island and Store Bælt.

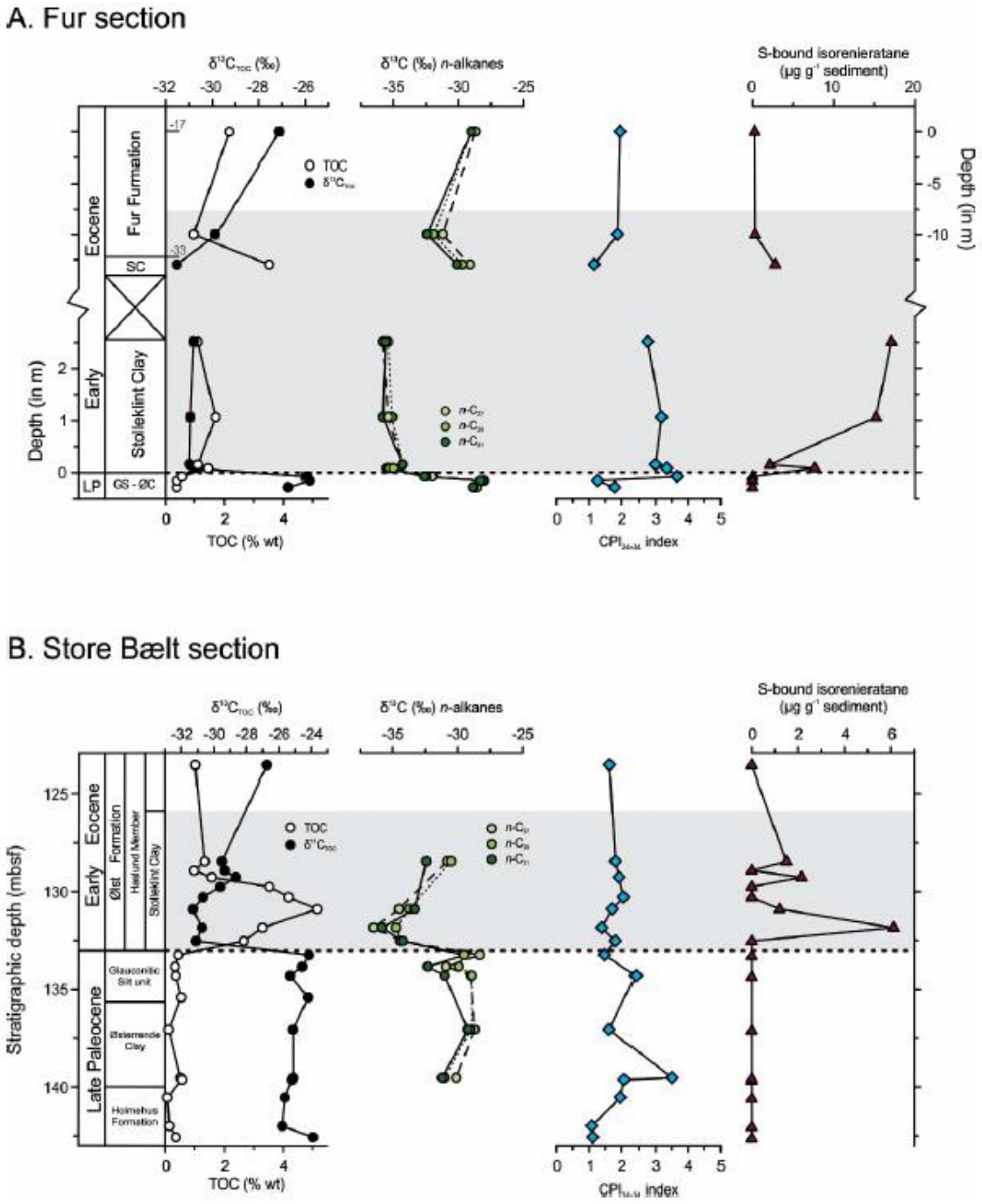

Figure 3: Profiles of the PETM sections at (A) Fur and (B) Store Bælt, showing the TOC content and the stable carbon isotopic composition of TOC, the stable carbon isotopic compositions of the C_{27} (light grey), C_{29} (middle grey), C_{31} (dark grey) *n*-alkanes, the Carbon Preference Index (CPI), and the abundance of S-bound isorenieratane. The dotted line indicates the onset of the CIE of the PETM and the grey area indicates the entire PETM interval. Note the different depth scale below and above the glacially-disturbed interval

described in the text. The ash layers -33 and -17 of Bøggild (1918) are shown. Abbreviations: LP= Late Palaeocene, GS = Glauconitic Silt unit, ØC = Østerrende Clay, SC = Stolleklint Clay.

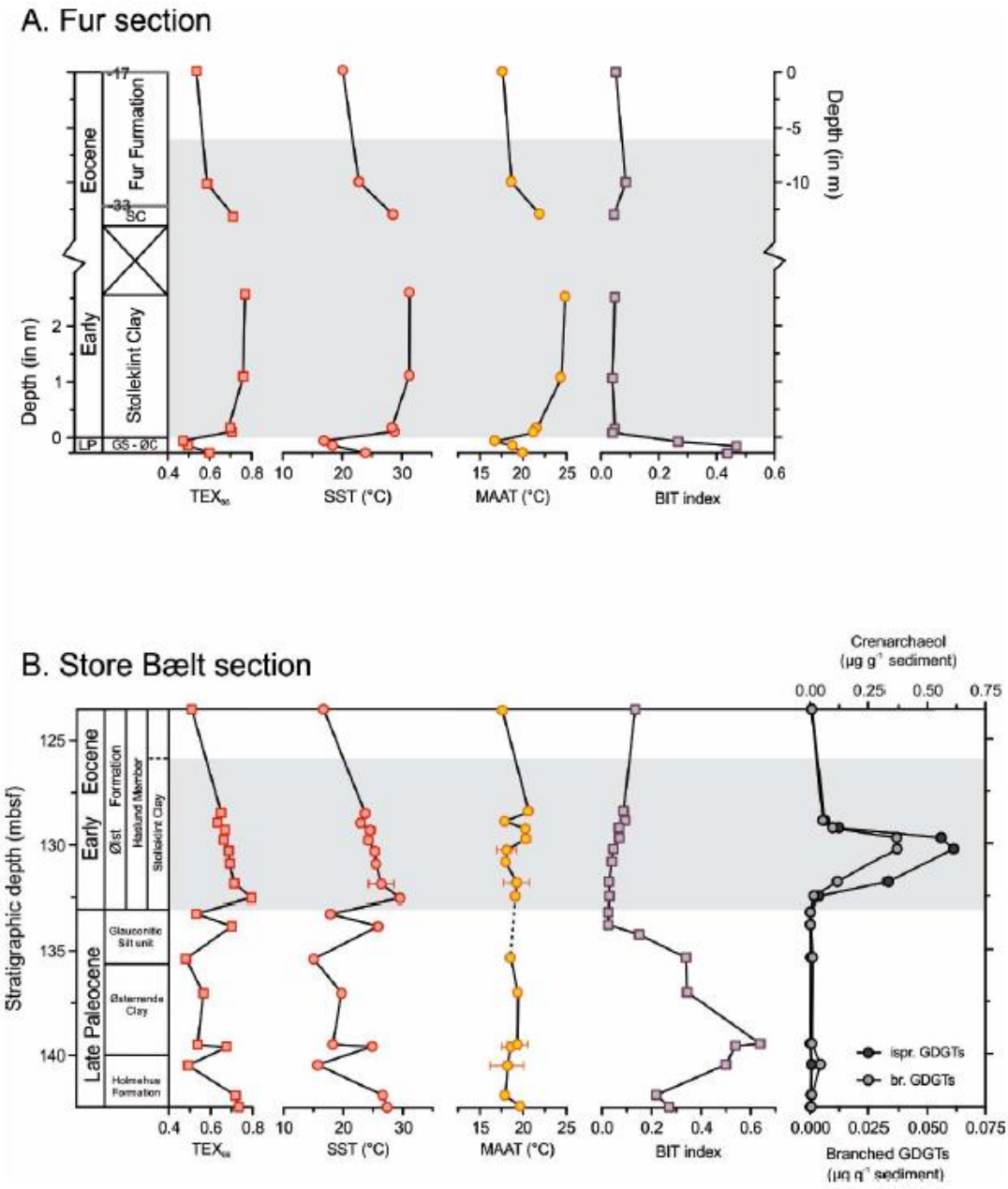

Figure 4: Profiles of the PETM sections at (A) Fur and (B) Store Bælt, showing the sea surface temperatures derived from TEX_{86} and mean annual air temperatures derived from the MBT'/CBT proxy, the BIT index, and absolute concentrations of crenarchaeol and branched GDGTs in µg g^{-1} sediment. Note the difference in scale for both, which differs by a factor of

ten. The dotted line indicates the onset of the CIE of the PETM and the grey area indicates the entire PETM interval. Note the different depth scale below and above the glacially-disturbed interval described in the text. The ash layers -33 and -17 of Bøggild (1918) are shown. Abbreviations: LP = Late Palaeocene, GS = Glauconitic Silt unit, ØC = Østerrende Clay, SC = Stolleklint Clay.